



Large Eddy Simulation of piloting effects on turbulent swirling flames

A.X. Sengissen, Alexis Giauque, Gabriel Staffelbach, M. Porta, W. Krebs, P. Kaufmann, Thierry Poinso

► To cite this version:

A.X. Sengissen, Alexis Giauque, Gabriel Staffelbach, M. Porta, W. Krebs, et al.. Large Eddy Simulation of piloting effects on turbulent swirling flames. Proceedings of the Combustion Institute, 2007, 31 (2), pp.1729-1736. <10.1016/j.proci.2006.07.010>. <hal-02148733>

HAL Id: hal-02148733

<https://hal.science/hal-02148733v1>

Submitted on 5 Jun 2019

HAL is a multi-disciplinary open access archive for the deposit and dissemination of scientific research documents, whether they are published or not. The documents may come from teaching and research institutions in France or abroad, or from public or private research centers.

L'archive ouverte pluridisciplinaire **HAL**, est destinée au dépôt et à la diffusion de documents scientifiques de niveau recherche, publiés ou non, émanant des établissements d'enseignement et de recherche français ou étrangers, des laboratoires publics ou privés.



Copyright - All rights reserved

Large Eddy Simulation of piloting effects on turbulent swirling flames

Sengissen A. X.^{*}, Giauque A. S.^{*}, Staffelbach G. S.^{*},
Porta M.^{*}, Krebs W.[†], Kaufmann P.[†] and Poinso T. J.[‡]

^{*} CERFACS, 42 Avenue G. Coriolis, 31057 Toulouse cedex, France

[†] Siemens PG, 45466 Mülheim an der Ruhr, Germany

[‡] Institut de Mécanique des Fluides de Toulouse, Avenue C. Soula, 31400 Toulouse, France

Abstract

Pilot flames, created by additional injectors of pure fuel, are often used in turbulent burners to enhance flame stabilisation and reduce combustion instabilities. The exact mechanisms through which these additional rich zones modify the flame anchoring location and the combustion dynamics are often difficult to identify, especially when they include unsteady hydrodynamic motion. This study presents Large Eddy Simulations (LES) of the reacting flow within a large-scale gas turbine burner for two different cases of piloting, where either 2 or 6 percent of the total methane used in the burner is injected through additional pilot flame lines. For each case, LES shows how the pilot fuel injection affects both flame stabilisation and flame stability. The 6 percent case leads to a stable flame and limited hydrodynamic perturbations in the initial flame zone. The 2 percent case is less stable, with a small-lift-off of the flame and a Precessing Vortex Core (PVC) in the cold stabilisation zone. This PVC traps some of the lean cold gases issuing from the pilot passage stream, changes the flame stabilisation point and induces instability.

Keywords: Combustion instabilities; Partially premixed; Swirled; Large Eddy Simulations

1. Introduction

Modern heavy duty gas turbines usually operate in lean premixed regimes to satisfy emissions regulations and can be very sensitive to combustion instabilities [1–3]. In most cases, flame stabilisation is provided by swirl injectors. A key zone of the chamber controlling instabilities is the burner outlet section

where swirl is very intense and must provide flame stabilisation. In these regions, the natural unstable modes of swirling flows (Precessing Vortex Cores or PVCs [4–8]) can interact with stabilisation and lift-off phenomena [9–12] to produce undesired oscillations.

A method to encourage robust stabilisation is to use small pilot flames in these regions, usually by adding pure fuel injection. This leads to increased NO_x lev-

els and therefore a compromise between stabilisation and pollution levels must be sought. Furthermore, stabilisation is a difficult task because its basic mechanisms in a piloted swirled zone are not well understood. Proof of the importance of fuel injection are observed in active control examples in which a small modulation of flow rate in the fuel lines feeding the pilot flame can be sufficient to alter the stability of the combustor [13–15].

Large Eddy Simulation (LES) is becoming a standard tool to study the dynamics of turbulent flames [16–18]. The objective of this paper is to use LES (section 2) to compare two different cases of piloting in a gas turbine burner. Either 2 or 6 percent of the total methane used in the burner is injected additionally through pilot fuel lines. The burner is described in section 3. The 6% pilot fuel case leads to a robust and stabilized flame while the 2% case induces a small lift-off zone of the flame where a PVC can develop and lead to flame oscillations (section 4).

Because of the complexity of the burner, no detailed measurements are available. However, observations in the full scale atmospheric test rig confirm LES predictions: the 2% leads to a more unstable flame than the 6% case.

2. Numerical approach used in Large Eddy Simulations

A fully compressible explicit code is used to solve the multi-species Navier-Stokes equations on hybrid grids [8, 19, 20]. Subgrid stresses are described by the classical Smagorinsky model [21]. A two-step chemical scheme is fitted for lean regimes on the GRI-Mech V3 reference [20]. The objective of the fit procedure is that the two-step mechanism and the GRI mechanism must produce the same flame speeds and maximum temperatures for laminar premixed one-dimensional flames for equivalence ratios ranging between $\phi = 0.4$ and $\phi = 1.2$.

The flame / turbulence interaction is modeled by the Dynamic Thickened Flame (DTF) model [22] which accounts for both mixing and combustion, and is crucial in partially premixed flames.

The explicit Lax-Wendroff numerical scheme uses second-order spatial accuracy and second-order time accuracy. The boundary condition treatment is based on a multi-species extension [19] of the NSCBC method [23], for which the acoustic impedance is controlled to minimise the unwanted reflections [24]. The adiabatic walls are handled using a logarithmic law-of-the-wall formulation which is known to perform well with the classical Smagorinsky model [25]. Typical runs are performed on a grid composed of 1.4 million tetrahedra on parallel architectures. Multiple validations of this LES tool are available for non-reacting [26, 27] and reacting flows [8, 20, 28, 29].

3. Target configuration

The test geometry is an axisymmetric combustion chamber (Fig. 1-a), with a 3MW full scale burner inlet (Fig. 1-b). This burner is composed of two coaxial swirlers:

- The premix passage swirler contains 24 vanes. Methane is injected through 10 small holes on each vane, ensuring efficient mixing and delivering approximately 90% of the total mass flow rate. In the LES, this flow is assumed to be fully premixed.
- The pilot passage swirler (detailed in the upper part of Fig. 1-b) delivers the remaining 10% of the flow rate (pure air). The central hub is connected to 8 vanes. Four additional tubes are inserted between the 8 vanes to inject the methane used for piloting.

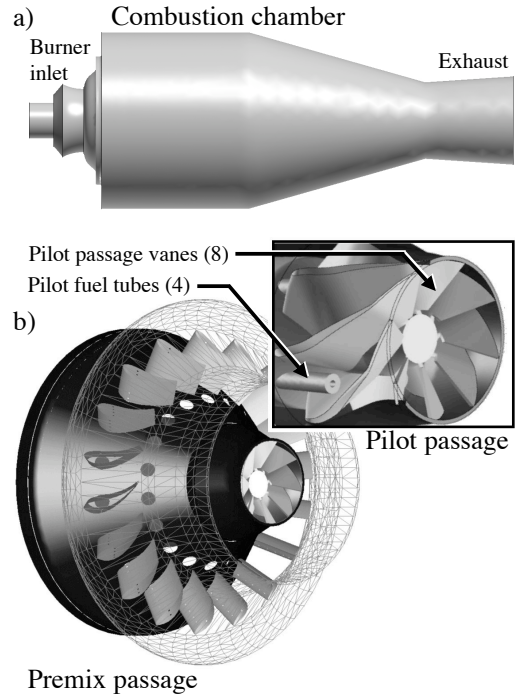


Fig. 1: a) Global view of the test geometry and b) zoom on the burner (pilot and premix passages) inner parts.

The computational domain includes all pilot passage vanes as well as the pilot fuel tubes, but not the premix passage vanes. Appropriate profiles of velocity and species are imposed to mimic the inlet experimental data [20] downstream of the premix passage vanes (Fig. 2).

The two operating points simulated in this study (2% and 6%) only differ by the fuel mass flow rates in the pilot fuel inlets:

- In the pilot passage stream, the fuel delivered by pilot injection leads to a global equivalence ratio of $\phi = 0.36$ (case 6%) and $\phi = 0.12$ (case 2%), of which the latter is outside the flammability

limits. However, the very heterogeneous mixture may allow combustion to develop locally in rich pockets or in diffusion flamelets, depending on the mixing efficiency.

- In the premix passage stream, the imposed profiles in both cases correspond to a perfectly premixed flow with an equivalence ratio of $\phi = 0.53$.

4. Results and discussion

In swirling flows, the general mechanism leading to flame stabilisation is well known [8, 20]: a central core of hot gases is maintained along the burner axis by the strong recirculation zone induced by swirl. This section shows how this classical stabilisation mechanism is affected by the pilot flames. Figures 3 and 5 respectively present statistical profiles (time averaged and RMS values) of temperature and axial velocity in the central plane. The axial location of these profiles is shown on Fig. 2. Velocity, temperature and location along axis are normalised respectively by references U_{ref} , T_{ref} and the pilot passage radius R .

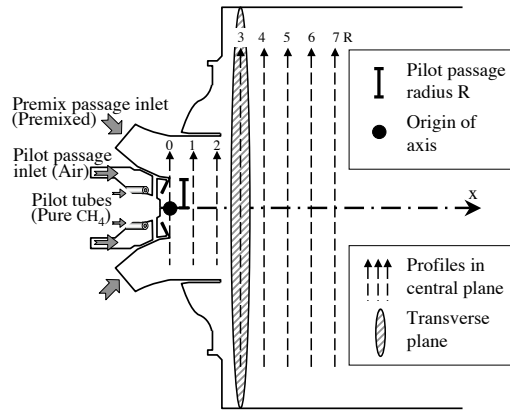


Fig. 2: Cross section of the test geometry and location of the planes used in Fig. 3, 5 and 8.

In the 6% pilot fuel case, the flame is clearly anchored on the central hub of the pilot passage, and the temperature fluctuations remain small (Fig. 3-b): burnt gases are found along the axis from $x = 0$ to $x = 2R$. Flame lift-off appears in the 2% case (Fig. 3-a). The gases between $x = 0$ and $x = 2R$ are cold. Hot pockets begin to appear after $x = 2R$ but they are very intermittent, as demonstrated by the very large values of the RMS temperature (error bars on Fig. 3-a). A clearer understanding of the differences between the two cases can be gained by plotting isosurfaces of temperature and stoichiometric equivalence ratio (Fig. 4). For the 6% case, the hot zone ($T = 2/3 \cdot T_{\text{ref}}$) is directly connected to the pilot passage hub (Fig. 4-b). For the 2% case, the flame is stabilised on a 'finger' of burnt gases which is rotating around the x-axis (Fig. 4-a), thereby inducing the

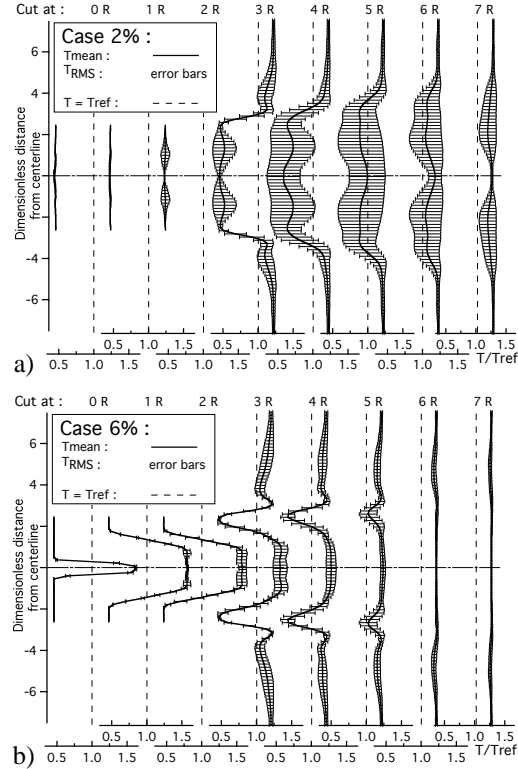


Fig. 3: Profiles of mean temperature (thick line), RMS of temperature (error bars) and $T = T_{\text{ref}}$ reference line (dashed line) for a) 2% case and b) 6% case.

large RMS fluctuations of temperature seen in Fig. 3-a.

The axial velocity fields (Fig. 5) also present significant differences. For the 6% case, a very large zone with small velocities (mean as well as RMS) develops between $x = 0$ and $x = 3R$ (Fig. 5-b). This zone contains the hot gases (Fig. 3-b) which provide stabilisation. The 2% case (Fig. 5-a) is characterised by a more intense recirculation (see for example cuts at $x = 2R$ or $x = 3R$) and a much higher level of RMS velocities. This zone (between $x = 0$ and $x = 3R$) contains cold gases (Fig. 3-a) which experience intense fluctuations. Even when the temperature increases (downstream of $x = 3R$), the velocity RMS values (Fig. 5-a) remain much higher for the 2% than for the 6% case, confirming that the 2% flame is not only lifted but also more hydrodynamically unstable.

Instantaneous combustion regimes can be visualised by scatter plots of reaction rate versus local mixture fraction Z (Fig. 6). In both cases, most reacting points are located very close to the global mixture fraction of the combustor Z_{mean} , but in the 6% case, combustion also takes place at richer regimes, even slightly above stoichiometric (Z_{st}), yielding higher maximum heat release. These points correspond to the roughly stoichiometric mixture issuing from the four pilot fuel jets after it has mixed with the premix

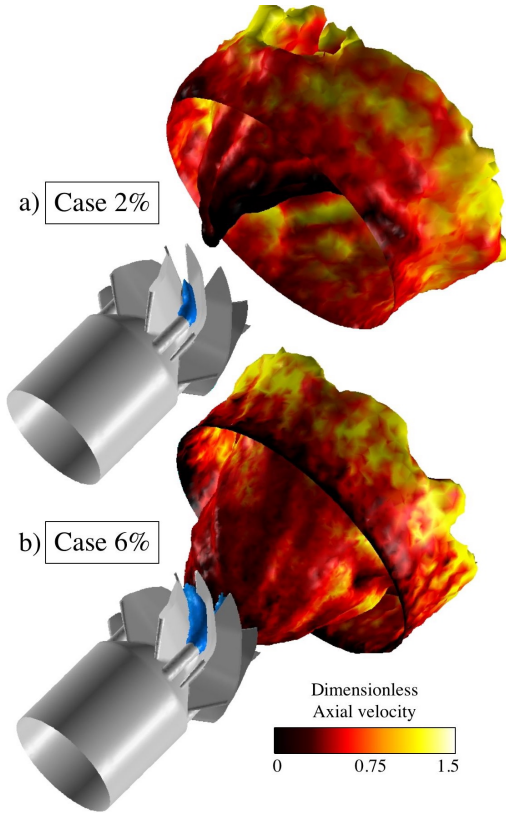


Fig. 4: Instantaneous isosurface of temperature ($T = 2/3 \cdot T_{\text{ref}}$, colored by axial velocity) and isosurface of equivalence ratio ($\phi = 1$, colored in blue) for a) 2% case and b) 6% case. **color figure in print**

passage air and passed through the vanes. By burning vigorously, these zones provide the robust stabilisation observed in Fig 4-b. For the 2% case, almost no combustion takes place above the mean mixture fraction Z_{mean} , indicating that the fuel injected in the pilot lines mixes too fast and cannot produce any significant diffusion flame zones which could provide stabilisation.

Typical instantaneous fields of equivalence ratio are displayed on Fig. 7. While the 6% case remains roughly axisymmetric and stoichiometric near the pilot passage hub, the 2% case in this zone has an asymmetric pattern below the flammability limit ($\phi < 0.4$), which rotates around the x-axis.

The near stoichiometric zone of Fig. 7-b for the 6% case is the source of the robust stabilisation of this regime: this allows the flame to propagate back to the burner and anchor to the hub. On the other hand, for the 2% case (Fig. 7-a), mixing between the pilot fuel and the pilot passage air is too fast and leads to a mixture at the pilot passage mouth which is too lean for flame propagation. Figure 7 also shows a zone within which the flow is reversed. This central recirculation zone is delimited by the white isoline $U = 0$. Note

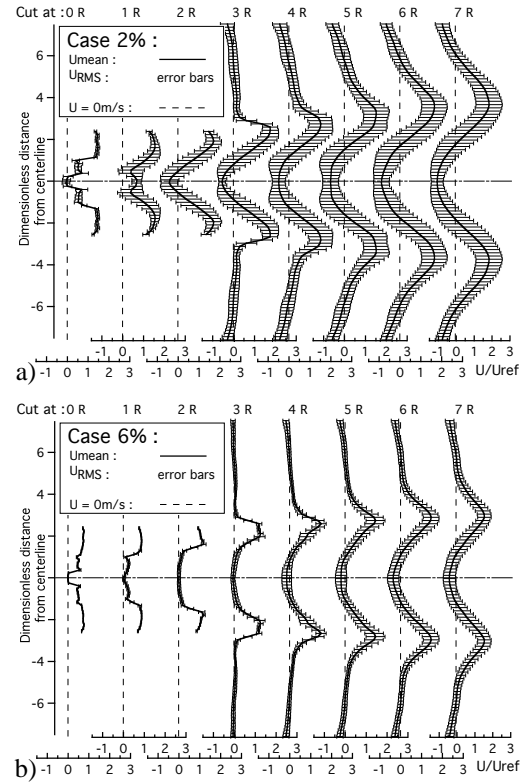


Fig. 5: Profiles of mean velocity (thick line), RMS of velocity (error bars) and $U = 0$ reference line (dashed line) for a) 2% case and b) 6% case.

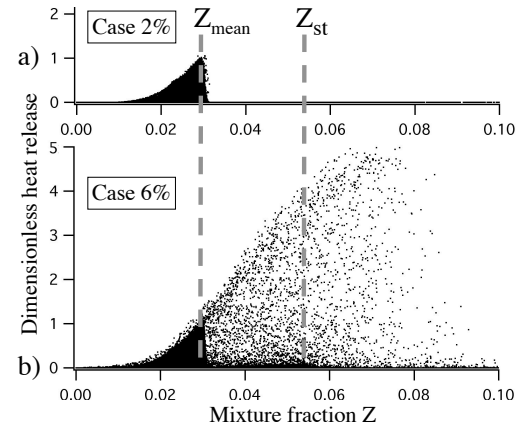


Fig. 6: Scatter plot of instantaneous heat release versus mixture fraction for a) 2% case and b) 6% case.

that the 6% case exhibits a smaller zone of reversed flow (as expected from the mean velocity profiles of Fig. 5) than the 2% case. Obviously, having reversed flow is not a sufficient criterion for stabilisation: having robust burning pilot flames is more important (as for the 6% case). For the 2% case, the absence of combustion in this zone leads to a lean cold region in

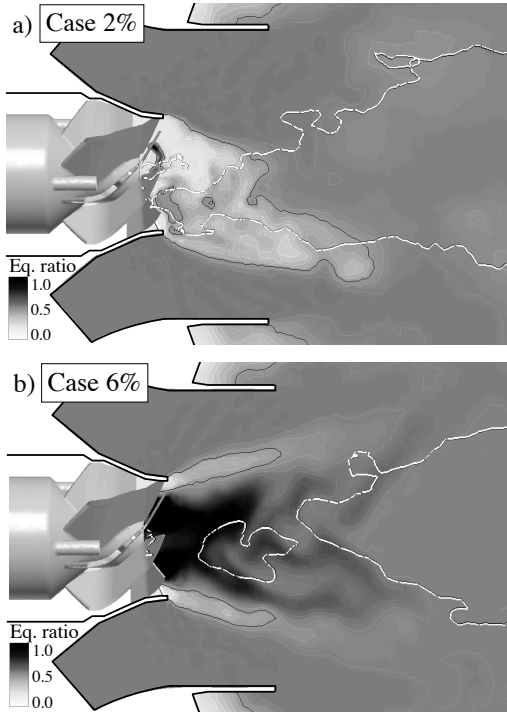


Fig. 7: Instantaneous field of equivalence ratio on central plane for a) 2% case and b) 6% case. Flammability zone ($\phi = 0.4$): black line. Recirculation zone ($U = 0$): white line.

which even reversed flow can not anchor the flame.

The existence of such a lean and cold zone leads to the formation of a PVC [4–8]. This PVC only occurs in the 2% case and precesses at 408Hz. The drastic change of velocity field near the pilot passage mouth for this case presented on Fig. 5 is one of the factors which most probably facilitate its development.

A specific feature of the 2% case is the correlation between the lean jet of methane and cold air issuing from the pilot passage and the low pressure zone due to the PVC structure. Figure 8 displays fields of pressure, temperature and local equivalence ratio (reconstructed through the mixture fraction) for both pilot fuel cases in a transverse plane at $x = 3R$.

The low pressure regions are a good indicator of the PVC presence (Fig. 8-a), and are well correlated with the cold (Fig. 8-b) and lean (Fig. 8-c) regions for the 2% case. The PVC appears to capture some of the lean cold gases produced by the pilot passage and prevents their mixing with the surrounding products. This observation is consistent with detailed mixing studies of jet / vortex interaction which show that mixing can be strongly decreased within vortex structures [30].

The flame then features a cold non-reacting "finger-like" rotating structure protruding within the stabilisation zone (illustrated by Fig. 4-a and sketched on Fig. 9). This is clearly not favorable either for

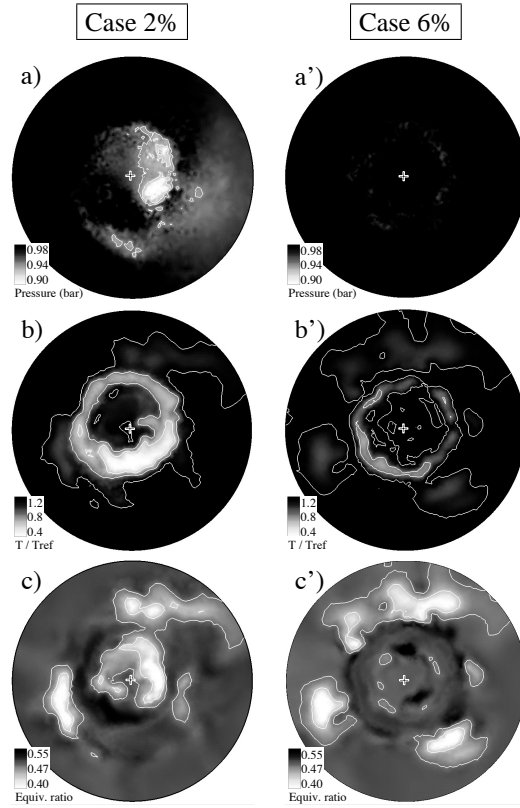


Fig. 8: Instantaneous fields of a) pressure, b) dimensionless temperature and c) equivalence ratio on transverse plane (see Fig. 2) for 2% case (left) and 6% case (right).

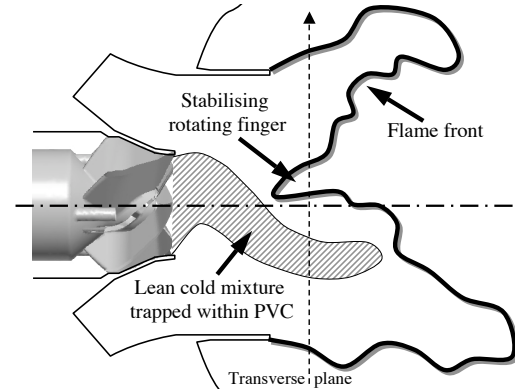


Fig. 9: Sketch of the finger-like rotating structure for the 2% case and location of the transverse plane (see Fig. 8).

flame stabilisation nor for thermoacoustic stability: RMS pressure levels for the 2% case can be as high as 6000 Pa (170 dB) on the axis and the noise is radiated to 2000 Pa (160 dB) at the wall while they do not exceed 500 Pa for the 6% case. For the 6% case, the situation is very different: a PVC is not observed (Fig. 8-a'), less cold gas reaches the plane at $x = 3R$ (Fig. 8-b') and lean gases are not found around the

axis (Fig. 8-c').

The mechanism leading to the PVC formation in the 2% case is purely due to hydrodynamic and combustion effects but not to acoustic coupling. A basic proof of the absence of acoustic coupling can be assessed by comparing the acoustic eigenfrequencies of the combustion chamber with the precessing frequency of the PVC (408 Hz). The fundamental transverse eigenmode is 575 Hz, and the non reflecting inlet/outlet treatment [24] is built to damp all the longitudinal modes.

5. Conclusions

This study presents Large Eddy Simulations (LES) of piloting effects in a full-scale gas turbine burner. By computing explicitly all details of the pilot passage zone where pure pilot methane is injected upstream of the vanes, LES provides new insights on the key mechanisms that control flame stability. When enough methane is injected in the pilot zone (in the 6% case), a roughly stoichiometric zone is formed at the burner mouth, allowing flame propagation within this zone and preventing the formation of a Precessing Vortex Core (PVC). On the other hand, when the flow rate of pilot fuel is too small (in the 2% case), the mixture issuing from the pilot passage is too lean, preventing flame stabilisation and leading to the formation of a PVC containing lean cold gases which diminishes the effect of piloting even more. Obviously, between the 2% and 6% piloting cases, a bifurcation takes place in the basic flow structure. The significant effects of this bifurcation captured by LES coincide with observations on stability limits in the full scale test rig.

Acknowledgments

This work was carried out with the support of Siemens PG in the framework of EC project DESIRE.

Most numerical simulations have been conducted on the computers of CINES, the French national computing center, on a SGI origin 3800.

References

- [1] W. Polifke, A. Fischer, T. Sattelmayer, *J. Eng. for Gas Turb. and Power* 125 (2003) 20–27.
- [2] V. Sankaran, S. Menon, *J. Turb.* 3 (2002) 011.
- [3] D. Smith, E. Zukoski, in: *21st Joint Propulsion Conference*, Monterey, 1985, pp. 85–1248.
- [4] P. Billant, J.-M. Chomaz, P. Huerre, *J. Fluid Mech.* 376 (1998) 183–219.
- [5] A. Gupta, D. Lilley, N. Syred, *Swirl flows*, Abacus Press, 1984.
- [6] M. Hall, *Ann. Rev. Fluid Mech.* 4 (1972) 195–217.
- [7] O. Lucca-Negro, T. O'Doherty, *Prog. Energy Comb. Sci.* 27 (2001) 431–481.
- [8] S. Roux, G. Lartigue, T. Poinsot, U. Meier, C. Bérat, *Combust. Flame* 154 (2005) 40–54.
- [9] Y. Mizobuchi, J. Shinjo, S. Ogawa, T. Takeno, *Proc. Combust. Inst.* 29 (2004) 2009–2015.
- [10] L. Muñoz, M. Mungal, *Combust. Flame* 111 (1–2) (1997) 16–31.
- [11] H. Pitsch, H. Steiner, *Phys. Fluids* 12 (2000) 2541–2554.
- [12] L. Vervisch, R. Hauguel, P. Domingo, M. Ruland, *J. Turb.* 5 (2004) 004.
- [13] C. Hantschk, J. Hermann, D. Vortmeyer, *Proc. Combust. Inst.* 26 (1996) 2835–2841.
- [14] K. McManus, T. Poinsot, S. Candel, *Prog. Energy Comb. Sci.* 19 (1993) 1–29.
- [15] T. Poinsot, D. Veynante, B. Yip, A. Trouvé, J.-M. Samaniego, S. Candel, *J. Phys. III* July (1992) 1331–1357.
- [16] H. Pitsch, *Ann. Rev. Fluid Mech.* 38 (2006) 453–482.
- [17] N. Peters, *Turbulent combustion*, Cambridge University Press, 2000.
- [18] T. Poinsot, D. Veynante, *Theoretical and numerical combustion*, R.T. Edwards, 2001.
- [19] V. Moureau, G. Lartigue, Y. Sommerer, C. Angelberger, O. Colin, T. Poinsot, *J. Comput. Phys.* 202 (2005) 710–736.
- [20] L. Selle, G. Lartigue, T. Poinsot, R. Koch, K.-U. Schildmacher, W. Krebs, B. Prade, P. Kaufmann, D. Veynante, *Combust. Flame* 137 (4) (2004) 489–505.
- [21] J. Smagorinsky, *Mon. Weather Review* 91 (1963) 99–164.
- [22] J.-P. L  gier, T. Poinsot, D. Veynante, in: *Summer Program 2000*, Center for Turbulence Research, Stanford, USA, 2000, pp. 157–168.
- [23] T. Poinsot, S. Lele, *J. Comput. Phys.* 101 (1) (1992) 104–129.
- [24] L. Selle, F. Nicoud, T. Poinsot, *AIAA Journal* 42 (5) (2004) 958–964.
- [25] W. Cabot, P. Moin, *Flow Turb. and Combustion* 63 (2000) 269–291.
- [26] C. Pri  re, L. Gicquel, A. Kaufmann, W. Krebs, T. Poinsot, *J. Turb.* 5 (2004) 1–30.
- [27] J. Schl  ter, *Int. J. Numer. Meth. Fluids* 18 (3) (2004) 235–246.
- [28] C. Martin, L. Benoit, F. Nicoud, T. Poinsot, *AIAA Journal* in press.
- [29] Y. Sommerer, D. Galley, T. Poinsot, S. Ducruix, F. Lacas, D. Veynante, *J. Turb.* 5 (2004) 037.
- [30] R. Paoli, F. Laporte, B. Cuenot, T. Poinsot, *Phys. Fluids* 15 (2003) 1843–1860.